ARCHIVIO ISTITUZIONALE DELLA RICERCA

Alma Mater Studiorum Università di Bologna
Archivio istituzionale della ricerca

Hierarchical electrospun tendon-ligament bioinspired scaffolds induce changes in fibroblasts morphology under static and dynamic conditions

This is the final peer-reviewed author's accepted manuscript (postprint) of the following publication:

Published Version:
Hierarchical electrospun tendon-ligament bioinspired scaffolds induce changes in fibroblasts morphology under static and dynamic conditions / Sensini A.; Cristofolini L.; Zucchelli A.; Focarete M.L.; Gualandi C.; de Mori A.; Kao A.P.; Roldo M.; Blunn G.; Tozzi G.. - In: JOURNAL OF MICROSCOPY. - ISSN 0022-2720. - ELETTRONICO. - 277:3(2020), pp. 160-169. [10.1111/jmi.12827]

Availability:
This version is available at: https://hdl.handle.net/11585/760027 since: 2021-03-02

Published:

DOI: http://doi.org/10.1111/jmi.12827

Terms of use:

Some rights reserved. The terms and conditions for the reuse of this version of the manuscript are specified in the publishing policy. For all terms of use and more information see the publisher's website.

This item was downloaded from IRIS Università di Bologna (https://cris.unibo.it/).
When citing, please refer to the published version.

(Article begins on next page)

20 April 2024

This is the final peer-reviewed accepted manuscript of:

J Microsc. 2020 Mar;277(3):160-169.

Epub 2019 Aug 2.

Hierarchical electrospun tendon-ligament bioinspired scaffolds induce changes in fibroblasts morphology under static and dynamic conditions

A Sensini, L Cristofolini, A Zucchelli, M L Focarete, C Gualandi, A DE Mori, A P Kao, M Roldo, G Blunn, G Tozzi

PMID: 31339556 DOI: 10.1111/jmi.12827

The final published version is available online at:

https://doi.org/10.1111/jmi.12827

Rights / License:

The terms and conditions for the reuse of this version of the manuscript are specified in the publishing policy. For all terms of use and more information see the publisher's website.

Hierarchical electrospun tendon-ligament bioinspired scaffolds induce changes in fibroblasts morphology under static and dynamic conditions

Alberto Sensini[1], Luca Cristofolini[1,2], Andrea Zucchelli[1], Maria Letizia Focarete[2,3], Chiara Gualandi[3,4], Arianna De Mori[5], Alexander Kao[6], Marta Roldo[5], Gordon Blunn[5], Gianluca Tozzi[6]

[1] Department of Industrial Engineering, Alma Mater Studiorum—University of Bologna, I-40131 Bologna, Italy

[2] Health Sciences and Technologies—Interdepartmental Center for Industrial Research (CIRI-HST), Alma Mater Studiorum—University of Bologna, I-40064 Ozzano dell'Emilia, Bologna, Italy

[3] Department of Chemistry 'G. Ciamician' and National Consortium of Materials Science and Technology (INSTM, Bologna RU), Alma Mater Studiorum—University of Bologna, I-40126 Bologna, Italy

[4] Advanced Mechanics and Materials – Interdepartmental Center for Industrial Research (CIRI-MAM), Alma Mater Studiorum—University of Bologna, I-40123 Bologna, Italy

[5] School of Pharmacy and Biomedical Science, University of Portsmouth – St Michael's Building, White Swan Road, Portsmouth PO1 2DT, United Kingdom

[6] Zeiss Global Centre, School of Mechanical and Design Engineering, University of Portsmouth, Portsmouth PO1 3DJ, United Kingdom

Corresponding author:
Gianluca Tozzi
Zeiss Global Centre
School of Mechanical and Design Engineering
University of Portsmouth
PO1 3DJ Portsmouth, United Kingdom
e-mail: gianluca.tozzi@port.ac.uk

Summary

The regeneration of injured tendons and ligaments is challenging since the scaffolds needs proper mechanical properties and a biomimetic morphology. In particular, the morphological arrangement of scaffolds is a key point to drive the cells growth to properly regenerate the collagen extracellular matrix. Electrospinning is a promising technique to produce hierarchically structured nanofibrous scaffolds able to guide cells in the regeneration of the injured tissue. Moreover, the dynamic stretching in bioreactors of electrospun scaffolds had demonstrated to speed up cell shape modifications *in vitro*. The aim of the present study was to combine different imaging techniques such as high-resolution x-ray tomography (XCT), scanning electron microscopy (SEM), fluorescence microscopy and histology to investigate if hierarchically structured poly(L-lactic acid) and collagen electrospun scaffolds can induce morphological modifications in human fibroblasts, while cultured in static and dynamic conditions. After 7 days of parallel cultures, the results assessed that fibroblasts had proliferated on the external nanofibrous sheath of the static scaffolds, elongating themselves circumferentially. The dynamic cultures revealed a preferential axial orientation of fibroblasts growth on the external sheath. The aligned nanofiber bundles inside the hierarchical scaffolds instead, allowed a physiological distribution of the fibroblasts along the nanofiber direction. Inside the dynamic scaffolds, cells appeared thinner compared with the static counterpart. This study had demonstrated that hierarchically structured electrospun scaffolds can induce different fibroblasts morphological modifications during static and dynamic conditions, modifying their shape in the direction of the applied loads.

Keywords:

Electrospinning, Hierarchical Scaffolds, High-Resolution X-Ray Tomography, Cell Culture, Dynamic Cell Culture, Cell Morphology, Tissue Engineering, Tendons and Ligaments.

Introduction

The challenge of the innovative three-dimensional scaffolds, suitable for tendon and ligament regeneration, is to strictly reproduce the native tissue mechanical properties and hierarchical morphology (Alshomer et al., 2018; Cheng et al., 2015; Goulet et al., 2014; Kuo et al., 2010). The morphological arrangement of the scaffold is fundamental to correctly drive cell proliferation and growth, during collagen extracellular matrix regeneration. It has been shown that fibroblasts and tenocytes shape is strictly dependent on the specific site of growth *in vivo*: cells that colonize tendon and ligament membranes (made of randomly arranged collagen fibrils), tend to spread their bodies; conversely, cells in the internal volume of these tissues appear elongated in the direction of the axially oriented fibrils (Kannus, 2000; Kastelic et al., 1978; Murphy et al., 2016). Several manufacturing approaches to produce fibrous scaffolds inspired to tendons or ligaments have been investigated in literature, among these electrospinning technology is the most promising (Sensini & Cristofolini, 2018). Thanks to the possibility to obtain nanoscale fibers with different spatial arrangements, electrospun scaffolds have demonstrated enhancement of cellular orientation in the fibers direction (Bosworth & Downes, 2011; Denchai et al., 2018). Furthermore, several studies have confirmed the possibility to speed up cell proliferation and elongation on the electrospun scaffolds with a simplified shape, such as flat mats, bundles or yarns, by uniaxially stretching the constructs in a bioreactor (Bosworth et al., 2014; Wu et al., 2017; Xu et al., 2014; Youngstrom & Barrett, 2016). These simple designs allow for convenient documentation of changes in cellular shape using standard techniques, such as scanning electron microscopy (SEM), fluorescent microscopy or histology. Despite the high-quality of images and the cellular information obtainable, these gold-standard methods have shown some limitation when applied to the study of the cell morphology on

complex three-dimensional scaffolds (Leferink et al., 2016). SEM images can achieve a high-resolution, but are limited to the surface of the structures. Fluorescent techniques, such as fluorescent or confocal microscopy, allow an accurate identification of the shape of cells, but are strongly limited by possible autofluorescent effects of the nanofibers, especially if they are composed by natural polymers such as collagen (Sensini et al., 2018). Moreover, these techniques do not allow easy visualization if the structure investigated is not planar, making the investigation of three-dimensional scaffolds challenging. On the other hand, histology allows a clear identification of the cellular components, even in case of three-dimensional shapes, but it typically produces a bi-dimensional view of the specimens and of the cells inside. This limits a correct definition of the cellular shape. Moreover, during the slicing and washing procedure, in particular for the electrospun materials, it is easy to damage parts of the scaffold losing the related information. A possible solution to overcome these limitations is offered by high-resolution x-ray computed tomography (XCT). However, due to the low X-ray attenuation of the polymeric nanofibers, XCT investigation of electrospun materials is particularly challenging. This problem is especially true in the case of collagenous materials (Balint et al., 2016; Zidek et al., 2016). Recent studies have defined dedicated protocols to overcome such limitations even in case of submicron voxel sizes (Bosworth et al., 2014; Sensini et al., 2018). Furthermore, Bradley et al. have defined a procedure to document, by using a laboratory XCT, cell infiltration inside electrospun mats of random microfibers (Bradley et al., 2017). However, to the best of our knowledge, no work has ever tried to investigate the cell growth and infiltration in complex three-dimensional electrospun nanofibrous scaffolds by combining XCT and other different imaging techniques. This approach could be fundamental to analyze how the different elements of the scaffolds can induce cellular morphological modifications.

The aim of the present study was to compare the fibroblast morphological modifications during static and dynamic culture protocols on complex electrospun scaffolds. Cells were seeded on three-dimensional electrospun nanofibrous hierarchically structured scaffolds made of a poly(*L*-lactic acid) (PLLA) and collagen (Coll) blend. Different imaging techniques including high-resolution x-ray tomography (XCT), scanning electron microscopy (SEM), fluorescent microscopy and histology were employed confirming different cellular modifications in shape and orientation during static and dynamic conditions of culture.

Materials and methods

In order to investigate the morphologically changes in the fibroblasts shape, electrospun PLLA/Coll nanofibrous hierarchically structured scaffolds were produced (Figure 1(A)). The scaffolds were seeded with human fibroblasts and cultured in different conditions for 7 days: two of each in static conditions, while the other two were stretched two times in a bioreactor for 1 hour each (Figure 1(B)). At the end of the culture, the specimens were cut in pieces and investigated with different imaging techniques (Figure 1(C)).

Hierarchical electrospun scaffolds production

In order to reproduce the morphology of tendon and ligament fibrils and fascicles (Kannus, 2000; Murphy et al., 2016), electrospun bundles (cross-sectional diameter = 550-650 μm) of aligned nanofibers (cross-sectional diameter of the nanofibers = 0.36±0.06 μm) of a PLLA/Coll-75/25 (w/w) blend were produced as previously described (Sensini et al., 2017, 2018). To obtain the bundles the following electrospinning parameters were used: a rotating drum collector (peripheral speed = 22.8 m s^{-1}); the polymer solution was delivered through two needles (internal diameter 0.51

mm); room temperature (RT) and relative humidity 20–30%; applied voltage = 22 kV; feed rate = 0.5 mL h^{-1}, electrospinning time = 2 hours; needles-collector distance = 200 mm; the sliding spinneret with the two needles had an excursion of 120 mm, with a sliding speed of 1200 mm min^{-1}.

To reproduce the structure of a whole tendon or ligament (Kastelic et al., 1978; Murphy et al., 2016), each bundle was pulled out from the drum, obtaining a ring-shaped structure that was twisted in the middle and bent over itself. Then, each assembly was covered with an electrospun epitenon/epiligament-like sheath, as previously described (WO 2018/229615 A1, 2018; Sensini et al., 2019; Sensini et al., 2019). The scaffolds were finally crosslinked with a mixture of *N*-(3-dimethylaminopropyl)-*N'*-ethylcarbodiimide hydrochloride (EDC) and *N*-hydroxysuccinimide (NHS) (Sigma-Aldrich, USA) as previously described (Alberto Sensini et al., 2018) (cross-sectional diameter = 1.46±0.08 mm; length of the scaffolds = 89.4±2.1 mm). Four hierarchical scaffolds were produced (Figure 1).

Cell seeding

The four hierarchical scaffolds were sterilized by immersion in 70% (v/v) ethanol (Acros Organics, Thermo Fisher Scientific, BEL) for 1 hour, washed in sterile PBS (Thermo Fisher Scientific, USA) three times to remove any remaining ethanol and equilibrated in complete medium for 24 hours. The complete medium was obtained by mixing Dulbecco Modified Eagle Medium (DMEM) (i.e. 4.5 g/L D-Glucose, with GlutaMAX™ and Pyruvate) (Thermo Fisher Scientific, USA), 10% foetal bovine serum (Thermo Fisher Scientific, USA) and 1% (v/v) penicillin/streptomycin solution (Thermo Fisher Scientific, USA).

Human foreskin fibroblasts (Hs27) were cultivated with complete medium at 37°C in a humid atmosphere with 5% CO_2. Medium was refreshed three times a week and cells were used between passage 4 and 6.

To perform the test, cells were seeded at 2.0 x 10^5 cells/scaffold. In particular, cells were suspended in 350 microliters of complete medium and seeded, using a syringe with a 25G needle: half volume was seeded on one side of the scaffold, then the scaffold was turned 180° and the other half volume was seeded on the other side. The seeding was carried out in a sterile petri dish. After 45 minutes in an incubator at 37°C and 5% CO_2, each hierarchical scaffold was transferred into one low adherence T25 flask each and covered with 5 ml of complete medium to allow for cell proliferation.

In order to avoid potential artefacts caused by the relevant amount of medium during the dynamic cultures (see below) and the total length of the specimens, quantitative data regarding the cell viability were not reported.

After 7 days of culture, the hierarchical scaffolds were fixed for 48 hours in 4% paraformaldehyde (PFA, Sigma-Aldrich, Saint Louis, USA) in PBS (at 4°C). Then, each specimen was cut in the center and divided in two equal sections: one half for the SEM/XCT imaging; the other was cut in two additional pieces for fluorescence microscopy and histology (Figure 1(C)).

Dynamic cultures in bioreactor

The dynamic culture was carried out on two hierarchical scaffolds by using a commercial bioreactor (MCB1, CellScale, CAN). Before each stretching session, the bioreactor was sterilized by washing the test chamber in ethanol 70% (v/v) and sterilized by means UV radiations under a fume hood for an hour. To transmit a uniaxial stretching, the hierarchical scaffolds were hooked between the stainless-steel actuator of

the bioreactor and a custom-made 3D printed pin of acrylonitrile butadiene styrene (ABS) (ABS-M30, Stratasys, USA). During each session, the specimens were covered with 150 ml of complete medium and stimulated for 1 hour with 4 mm of displacement (corresponding at a strain of approximately 5%) at a frequency of 1 Hz (3600 cycles). These parameters were chosen in accordance with the literature (Bosworth et al., 2014). Each of the two scaffolds was stretched two times during the 7 days of culture (i.e. at day three and day six of culture). After each bioreactor session, the dynamic specimens were put in T25 flasks with 5 ml of medium and left in static conditions for two days.

Static cultures

Parallelly, as a control for the dynamic specimens, two hierarchical scaffolds were cultured for 7 days in T25 flasks with 5 ml of medium, changing the medium at day 3 and six of culture.

High-resolution x-ray tomography

To evaluate the full-field fibroblast distribution, morphology and the hierarchical arrangement in the scaffolds, an XCT investigation was performed.
Firstly, after fixing with PFA, the scaffolds specimens for XCT were washed three times in PBS. Specimens were post-fixed with osmium tetroxide (Sigma-Aldrich, USA) for 1 hour and then dehydrated in ethanol (v/v) 30%, 50%, 70%, 90%, 95% and 100% for 1 hour for each step (the 100% step was repeated twice). Then the specimens were dehydrated in acetone for 20 minutes. The specimens were chemically dried using a mixture of hexamethyldisilazane (HMDS) (Sigma-Aldrich, USA) and ethanol in different (v/v) ratios: (i) HMDS:ethanol = 1:2 (v/v) and (ii) HMDS:ethanol = 2:1 (v/v) for 20 minutes each. An additional step was performed in HMDS 100% until dry.

To avoid imaging artifacts resulting from micromovements, the specimens were fixed in custom-made plastic masks adapted from (Sensini et al., 2018).

The two dynamic and static specimens of the hierarchical scaffolds were scanned with a laboratory XCT system (Xradia 520 Versa, Zeiss X-ray Microscopy, USA), with the following parameters:

(i) Voxel size = 1.6 micrometers (i.e. overview of the specimens): 40 kV voltage, 2 W power, 49 microampere tube current, 10 sec. exposure time.

(ii) Voxel size = 0.5 micrometers (i.e. zoom-in on the fibroblasts): 40 kV voltage, 2 W power, 50 microampere tube current, 30 sec. exposure time.

All the XCT images, were reconstructed using the Scout-and-Scan Reconstructor software (Zeiss, USA), and were visualized using XM3DViewer1.2.8 software (Zeiss, USA).

SEM imaging

After the XCT investigation, in order to confirm the fibroblasts presence, the XCT specimens were removed from the masks and prepared for the SEM imaging. Each specimen was cut in two pieces: one was longitudinally opened with a scalpel to investigate the fibroblasts on the internal bundles, while the other was left intact to investigate the fibroblasts on the electrospun sheath. Scanning Electron Microscopy (SEM) (Philips 515 SEM, NL) observations were carried out using an accelerating voltage of 15 kV and specimens were gold sputtered.

Directionality analysis

In order to quantify the orientation of the nanofibers of the scaffolds, the Directionality plugin of ImageJ was used (Liu, 1991; Schindelin et al., 2012; Schneider et al., 2012). This approach quantifies the distribution of nanofibers within a given angle from the axis of the specimen. The analysis was performed using a Local Gradient Orientation method following a procedure previously applied (Sensini et al., 2018).

To assess the orientation of the bundles inside the hierarchical assemblies, a full volume investigation was performed applying the procedure to all the slices of the XCT stack (voxel size = 1.6 micrometers), after reslicing. In order to list also the orientation of the nanofibers in a single crosslinked PLLA/Coll-75/25 bundle, the Directionality analysis data on a XCT scan from a previous study were reported (Sensini et al., 2018).

To quantify the orientation of the nanofibers in the electrospun sheath the Directionality analysis was performed on a stack of 5 SEM surface images (magnification = 8000x) derived from (Sensini et al., 2018).

In order to investigate the preferential orientation of the fibroblasts on the external sheath, in static and dynamic conditions of culture, a Directionality investigation was performed on a stack of 2 fluorescent images for each condition of culture (see below) (magnification = 20x) derived and adapted from (Sensini et al., 2018; Tseng et al., 2013). As the nuclei are better visible and are stretched in the same direction of the cell itself, the analysis was based on the alignment of the nuclei. Firstly, to enhance visibility of the cells nuclei the fluorescent images were segmented, using ImageJ. Over each segmented image, a mask was produced onto which lines were drawn of the same length and orientation of the longest axis of each nucleus. Finally, the masks were analyzed with Directionality as described above.

Fluorescent microscopy

After PFA fixing, specimens were washed with PBS and put in 3 ml of Triton-X (Sigma-Aldrich, USA) 0.1% (v/v) for 15 min. Then, the scaffolds were washed 3 times with PBS, before being treated with 1% (v/v) bovine serum albumin (BSA) (Sigma-Aldrich, USA) in PBS, for 1 hour. Then, the specimens were washed twice with sterile PBS. Phalloidin Dylight 550 (Thermo Fisher Scientific, USA) (2 units/ml in PBS) was added to each sample before incubation for 90 min at RT. Then the specimens were washed two times with PBS and DAPI (Sigma Aldrich, USA) (2 µg/ml) was added and incubated for 20 min in the dark, at RT. The specimens were stored at 4°C in petri dishes containing sterile PBS to prevent specimen dehydration. Finally, the external surfaces of the were imaged using a fluorescent microscope (Axio Imager Z1, Zeiss, USA) equipped with a camera (Hamamatsu HR, Hamamatsu, JAP) and a color camera (AxioCam MRc, Zeiss, USA) too. Images were processed by Volocity 6.3 software (Quorum Technologies Inc, UK).

Histology

The specimens for the haematoxylin and eosin staining were fixed in 4% (v/v) PFA/PBS overnight. PFA fixed specimens were processed into paraffin (Histosec®, Merck, Darmstadt, GER), using a dedicated embedder (EG1150 H, Leica, Wetzlar, GER) and sectioned (slices thickness = 5 µm) using a microtome (RM2235, Leica, GER). The specimens were sectioned parallelly to their longitudinal axis. Sections were deparaffinized and incubated in hematoxylin (Sigma-Aldrich, USA) and then in alcoholic eosin (Sigma-Aldrich, USA) for 5 min respectively. Finally, sections were differentiated, dehydrated in graded series of ethanol, and mounted in dibutyl phthalate xylene (DPX) (Sigma-Aldrich, USA) using glass coverslips. The histological slices of the scaffolds were imaged using a microscope (Diaplan, Leitz, GER) and processed with the Image-Pro Plus 6 software (Media Cybernetics, UK).

Cell morphology

In order to quantify the dimensions of cells (the length, i.e. the preferential direction of elongation of the cellular body; and the width and thickness), in the different conditions of culture, measurements of cells bodies were performed using ImageJ on the different images acquired. The cells length and width were estimated from XCT, fluorescence, SEM and histological images (static cultures: n = 20 cells for the length; n = 27 cells for the width; dynamic cultures: n = 8 cells for the length; n = 4 cells for the width), while the cells thickness was measured using SEM and histological images (static cultures: n = 7 cells; dynamic cultures: n = 5 cells). The mean (three measurements for each cell) of each parameter was used to produce the final mean and standard deviation of each dimension.

Results

Morphological investigation of the hierarchical scaffolds

To investigate the orientation of the nanofibers and bundles in the different levels of the hierarchical scaffolds, a Directionality analysis was performed (Figure 2). The Directionality analysis confirmed the preferential axial orientation of the nanofibers in the bundles, with a predominant peak of 31.4 ± 2.82% in the range of 0°-3° from the bundle axis, and a decrescent distribution (Sensini et al., 2018). A small amount of nanofibers (0.55 ± 0.08%) was perpendicular to the bundle (87°-90°). The Directionality investigation showed that the nanofibers of the sheaths for the hierarchical assemblies had a slight preferential circumferential orientation: more than 31% of the nanofibers fell in the range of 66°-90°. The preferential axial of alignment of the bundles inside the

hierarchical scaffolds was confirmed by a predominant peak of 61.6% ± 9.43% in the range of 0°-3°, and a decrescent distribution.

Fibroblasts morphology from XCT investigation

The specimens mounting setup for the XCT scans successfully prevented the artefacts of micromovements, permitting to obtain high-resolution images after the three-dimensional reconstruction (Figure 3). The hierarchical scaffolds were homogeneous, and the internal bundles strongly grouped by the electrospun sheath. The cells fixation and dehydration procedure enabled visualization of the fibroblasts growth on the hierarchical scaffolds (Figure 3). The reconstructions with a 1.6 µm voxel size provided an overview of the specimens (Figure 3(A)). Zooming on the sheath at 0.5 µm voxel size, fibroblasts were clearly distinguishable (Figure 3(B)). On the sheath of static specimens, fibroblasts were circumferentially oriented along the axis of the scaffolds, spreading their bodies also along the scaffold longitudinal axis (Figures 3(AI, AII) and 3(BI, BII)). On the sheath of dynamic specimens, the fibroblasts were thinner and less wide (see below), with increasing axial orientation compared to the static ones (Figure 3(AIII, AIV) and 3(BIII, BIV)). In the internal bundles, due to the high-alignment of the nanofibers and the elongated shape of the fibroblasts, cell detection was not possible.

Fibroblasts morphology from SEM investigation

The SEM images obtained for the same specimens used for the XCT scans and are shown in Figure 4. Despite the preferential random arrangement of the sheath nanofibers, the static fibroblasts showed a circumferential orientation with spread bodies (Figure 4(AI, II)), while cells on the dynamic specimens were thinner and preferentially elongated axially to the hierarchical scaffolds (Figure 4(BI, II)). The SEM investigation also assessed the fibroblasts infiltration inside the hierarchical scaffolds, both in static

and dynamic conditions. In both test conditions the internal fibroblasts appeared elongated and distributed axially aligned with the bundles nanofibers (Figure 4(AIII, AIV) and (BIII, BIV)). In the dynamic specimens the fibroblast appeared thinner compared to the static counterpart (Figure 4(BIII, IV)).

Fibroblasts morphology from fluorescence microscopy investigation

The fluorescence microscopy results are reported in Figure 5. On the static specimens, fibroblasts were again circumferentially oriented on the nanofibrous sheath (the nuclei were also ovalized in the transversal direction of the scaffolds), with spread bodies (Figure 5(A)). In the sheath of dynamic specimens, the fibroblasts appeared more axially aligned compared with the static ones (Figure 5(B)).

The Directionality analysis of the cell nuclei performed on the electrospun sheaths revealed that, in static specimens, the 71.1% of cells were oriented in a range of 72°-90° (Figure 6). In the dynamic specimens instead, the 53.4% of cells were oriented in the range of 0°-18° (Figure 6).

The fluorescence investigation in the internal bundles was not possible due to a low infiltration of the fluorescent reagents.

Fibroblasts morphology from histological investigation

The histological investigation outcomes are showed in Figure 6. The axial slices of the hierarchical scaffolds obtained, had cut transversally the fibroblasts grown on the electrospun sheaths (Figure 7(AI, II) and 7(BI, II)). In both the static and dynamic specimens, the fibroblasts appeared preferentially circumferentially arranged, due to the reduced axial elongation of their bodies. Moreover, on the dynamic specimens, the fibroblasts were thinner than on the static ones (according to their progressive extension

312 in the axial direction). Cells also infiltrated inside the hierarchical scaffolds aligning
313 themselves in the nanofibers direction (Figure 7(AIII, IV) and 7(BIII, IV)). The
314 fibroblasts in the dynamic specimens appeared thinner compared with the static
315 counterpart.

316 *Quantification of cells morphology*

317 The quantification of cells morphology revealed that in the static specimens, the cells
318 on the electrospun sheaths had a length of 72.1±27.9 micrometers, a width of 18.8±15.3
319 micrometers and a thickness of 3.2±0.8 micrometers; in the internal bundles, the cells
320 showed a length of 26.8±9.9 micrometers, a width of 2.5±1.6 micrometers and a
321 thickness of 1.5±0.2 micrometers. In the dynamic specimens, the cells on the sheath had
322 a length of 77±52.4 micrometers, a width of 8.9±6.9 micrometers and a thickness of
323 1.9±0.6 micrometers; on the internal bundles the cells had a length of 21.4±8.5
324 micrometers, a width of 2.6±1.3 micrometers and a thickness of 1.2±0.8 micrometers.

325 **Discussion**

326 To produce an electrospun scaffold suitable for tendon and ligament tissue engineering,
327 proper mechanical properties need to be combined to a biomimetic hierarchical
328 structure. These properties are mandatory to transmit physiological loads to the cells,
329 enabling their proper infiltration and growth inside the scaffolds. The aim of this study
330 was to investigate an innovative electrospun PLLA/Coll-75/25 hierarchically structured
331 scaffold, using different imaging techniques, in order to evaluate its ability to guide the
332 fibroblasts growth in static and dynamic conditions. The hierarchical scaffolds were
333 assembled by wrapping a PLLA/Coll-75/25 ring-shaped bundles of axially aligned
334 nanofibers, with an electrospun PLLA/Coll-75/25 sheath of randomly oriented

nanofibers. The scaffolds nanofibers and bundles were in the same size range of collagen fibrils and fascicles reported in literature (Kastelic et al., 1978). The Directionality analysis confirmed that bundles nanofibers, as well as bundles themselves, were axially aligned with the hierarchical scaffolds, while the nanofibers of the sheath showed a slightly circumferential orientation (Figure 2). In this way the hierarchical structure of a whole tendon or ligament was reproduced (Kastelic et al., 1978; Murphy et al., 2016). In order to evaluate the morphological changes in the cell shape induced by the hierarchical scaffolds, Hs27 fibroblasts were seeded on them for 7 days, comparing a static culture with a dynamic one in a bioreactor. To reproduce a physiological displacement configuration, the stretching parameters of the bioreactor were chosen consistently with the previous literature (Bosworth et al., 2014). At the end of the cultures, the full-field XCT investigation permitted to successfully visualize the fibroblasts grown on the external sheaths (Figure 3). Considering such complex and three-dimensional nanofibrous scaffolds, acquiring XCT images was challenging. In their work, Bradley et al. (Bradley et al., 2017) were able to visualize human fibroblasts seeded on electrospun poly(lactide-*co*-glycolide) (PLGA) random microfibrous mats by using a laboratory XCT scanner thanks to the micrometric cross-section of the fibers and the different levels the X-rays attenuation between the PLGA and the cellular component. In the case of the PLLA/Coll nanofibers instead, it is difficult to obtain tomographic images fibers, due to the low absorption of the collagen of X-rays (Balint et al., 2016; Zidek et al., 2016). This criticality is increased when the aim of the XCT scan is to discriminate elements with a similar attenuation and dimensions, such as cells and collagenous nanofibers. This aspect was fundamental for the XCT visualization of fibroblasts. Due to their spread shape and the random arrangement of the nanofibers, fibroblasts detection on the electrospun sheath was clearly visible (Figure 3(B)).

360 Conversely, the identification of cells inside the internal bundles was not distinguishable
361 (Figure 3(AII) and 3(AIV)). This was mainly caused by the axially aligned nanofibers
362 and the thinner and elongated shape of the cells. Further optimization, especially in the
363 thresholding phase would possibly to allow the XCT detection of cells along the bundles
364 aligned nanofibers.
365 In order to overcome this limitation and to validate the XCT results, additional imaging
366 techniques such as fluorescence microscopy, SEM and histology were performed. The
367 combination of these imaging protocols confirmed that fibroblasts on the electrospun
368 sheath of the scaffolds adopt a different shape depending on the culture conditions
369 employed. Both on the static and on the dynamic specimens, the cells had a length that
370 was one order of magnitude longer than the other two dimensions. On the electrospun
371 sheath of the static specimens, cells were elongated along the circumference of the
372 scaffolds with a spread body, while in the dynamic ones, a prevalent axial orientation
373 with thinner and slender morphology was observed (Figures 3-5 and Figure 7).
374 Moreover, the SEM and histological investigations showed that fibroblasts were able to
375 penetrate inside the electrospun sheath, growing and aligning themselves in the direction
376 of the axially aligned nanofibers. In the dynamic specimens, the cells bodies were
377 slightly thinner and shorter (length = 21.4±8.5 micrometers; thickness = 1.2±0.8
378 micrometers) compared to the static ones (length = 26.8±9.9 micrometers; thickness =
379 1.5±0.2 micrometers) (Figures 4, 5 and Figure 7). These results were in accordance with
380 the previous studies on cell cultures carried out on PLLA/Coll electrospun bundles of
381 aligned nanofibers (Sensini & Cristofolini, 2018; Sensini et al., 2018).
382 However, considering the different imaging investigations, the fibroblasts grown on the
383 sheath of the hierarchical scaffolds showed an unprecedented phenomenon compared to
384 previous cell studies (Alshomer et al., 2018; Hampson et al., 2008; Sensini &

385 Cristofolini, 2018). In fact, the circumferential alignment and elongation of cells grown
386 in the static condition was unexpected, even considering the slightly circumferential
387 alignment of the sheath nanofibers (Figure 2). Moreover, when cultured under dynamic
388 conditions, the sheath fibroblasts progressively elongated their shape trying to align
389 themselves to the axis of the hierarchical scaffolds. All these qualitative considerations
390 about the cellular orientation, were confirmed by the cellular Directionality analysis
391 performed on cells grown on the sheaths in the different conditions of culture (Figure
392 6). This behavior can be probably ascribed to the combination of three factors: the
393 electrospinning production process of the sheath, the hydration and mechanical
394 component, and the crosslinking of the nanofibers. Firstly, the mechanism to produce
395 the sheath was proved to tune the level of compacting of the internal bundles of the
396 hierarchical scaffolds (WO 2018/229615 A1, 2018; Sensini et al., 2019; Sensini et al.,
397 2019). This effect causes a pre-tensioning of the sheath nanofibers and of the internal
398 bundles. Secondly, after immersion in the culture medium, the scaffolds absorbed the
399 liquid which likely resulted in swelling of the internal bundles inducing additional
400 stretching of the sheath. The combination of these two effects can explain the presence
401 of circumferential stress, that could in turn drive the fibroblasts to change shape even in
402 static conditions. The progressive axial alignment of cells in the dynamic cultures
403 instead, could be explained by considering the effect of the collagen crosslinking. In
404 fact, it is possible that, during the crosslinking process, the nanofibers at the interface
405 between the sheath and the internal bundles could have been crosslinked together,
406 reducing their sliding. This could have caused a transmission of the axial load between
407 the bundles and sheath, producing an increment of the longitudinal stretch of the sheath
408 themselves, that induced the cells alignment. Both these effects, to the best of our

knowledge, were completely unexplored so far and they need further investigations in the near future increasing the sample size of the hierarchical scaffolds tested.

Conclusion

In this study a preliminary investigation on the change in fibroblasts morphology was assessed by culturing them on electrospun hierarchical scaffolds in static and dynamic conditions. The integration between XCT scans and gold-standard techniques such as SEM, fluorescence microscopy and histology allowed the detection of the modifications in the cell morphology and orientation. Considering the results, these electrospun hierarchical scaffolds could be suitable for future *in vivo* animal study, permitting an axial orientation of cells both on the electrospun sheath and the internal bundles when stimulated with axial loads. Moreover, the improvement of the imaging protocols developed in this study will be useful for the future development of correlative microscopy workflows dedicated to similar electrospun materials.

Acknowledgments

The Italian Ministry of University and Research (MIUR) is acknowledged. The mobility of Alberto Sensini was funded by the University of Bologna (Marco Polo grant). Type I collagen was kindly provided by Kensey Nash Corporation d/b/a DSM Biomedical (Exton, USA). The Zeiss Global Centre at the University of Portsmouth is greatly acknowledged for the support in X-ray imaging and data post-processing. The project was partially funded by the University of Portsmouth through a Research and Innovation Development Fund. The authors greatly acknowledge CellScale and Jim Veldhuis for technical training of Alberto Sensini in the use of the bioreactor. The authors acknowledge Carlo Gotti and Marina Fichera for the help during the scaffolds production and the imaging post processing. Marco Curto, Martino Pani and Robin

Rumney were also gratefully acknowledged for the help and suggestions in the design of the 3D-printed parts, design tables reviewing, and the cell culture planning. The authors also gratefully acknowledge Sabrina Valente and Gianandrea Pasquinelli for the useful suggestions and the use of the facilities during the histologic investigations.

Figure captions

Fig. 1. Workflow of the experiment. (A) Electrospun hierarchical scaffolds assembly (scale bar = 1 mm). (B) Fibroblasts culture: two scaffolds were cultured in static conditions, while other two with uniaxial sessions of stretching in a bioreactor. (C) Scaffolds preparation for the different imaging investigations (scale bar = 1 mm).

Fig. 2. Directionality analysis at different levels of the hierarchical scaffolds. The directionality histograms show the comparison between: the alignment of the bundles inside the hierarchical scaffold (gray bars), the distribution of nanofibers in the different directions for the bundle (green bars) and on the electrospun sheath (blue bars). An angle of 0° means that the nanofibers were aligned with the longitudinal axis of the hierarchical scaffold, an angle of 90° means that the nanofibers were perpendicular to it. Mean and standard deviation between images of the same specimen are plotted.

Fig. 3. XCT images of fibroblasts cultured onto the hierarchical scaffolds in static (I, II) and dynamic (III, IV) conditions. (AI, III) Overview of the scaffolds; (AII, IV) superficial crop showing the internal bundles (voxel size = 1.6 micrometers; scale bar =1 mm). (BI, III) Overview of fibroblasts on the external sheath; (AII, IV) zoom on the fibroblasts (voxel size = 0.5 micrometers; scale bar = 200 micrometers).

Fig. 4. SEM images of fibroblasts cultured onto the hierarchical scaffolds in static (A) and dynamic (B) conditions (scale bar = 10 micrometers). (I-II) SEM images of the fibroblasts on the electrospun sheath; (III-IV) SEM fibroblasts on the internal bundles.

Fig. 5. Fluorescence images of fibroblasts onto the hierarchical scaffolds sheath in static (A) and dynamic (B) conditions (scale bar = 30 micrometers).

Fig. 6. Directionality analysis of cells grown on the electrospun sheaths (based on the orientation of the cells nuclei) in static and dynamic conditions of culture. An angle of 0° means that the cells were aligned with the longitudinal axis of the hierarchical scaffold, an angle of 90° means that the cells were perpendicular to it. Mean and standard deviation between images of the static and dynamic specimens are plotted.

Fig. 7. Histological investigation on the hierarchical scaffolds cultured in static (A) and dynamic (B) conditions (scale bar = 50 micrometers). (I-II) Zoom-in on the fibroblasts on the electrospun sheath; (III-IV) images of the elongated fibroblasts on the aligned nanofibers of the internal bundles.

References:

Alshomer, F., Chaves, C., & Kalaskar, D. M. (2018). Advances in Tendon and Ligament Tissue Engineering : Materials Perspective. *J. Mater.*, ***2018***, 1–18. https://doi.org/10.1155/2018/9868151

Balint, R., Lowe, T., & Shearer, T. (2016). Optimal contrast agent staining of ligaments and tendons for X-ray computed tomography. *PLoS One*, ***11***(4). https://doi.org/10.1371/journal.pone.0153552

Bosworth, L. A., Rathbone, S. R., Bradley, R. S., & Cartmell, S. H. (2014). Dynamic loading of electrospun yarns guides mesenchymal stem cells towards a tendon lineage. *J. Mech. Behav. Biomed. Mater.*, ***39***, 175–183. https://doi.org/10.1016/j.jmbbm.2014.07.009

Bosworth, L. A., & Downes, S. (2011). *Electrospinning for Tissue Regeneration*. (Lucy A. Bosworth & S. Downes, Eds.). Cambridge: Woodhead Publishing. https://doi.org/10.1016/B978-1-84569-741-9.50001-X

Bradley, R. S., Robinson, I. K., & Yusuf, M. (2017). 3D X-Ray Nanotomography of Cells Grown on Electrospun Scaffolds. *Macromol. Biosci.*, ***17***(2), 1–8. https://doi.org/10.1002/mabi.201600236

Cheng, M. T., Shih, Y. R. V., & Lee, O. K. (2015). Tendon and Ligament Tissue Engineering. In A. Vishwakarma, P. Sharpe, S. Shi, & M. Ramalingam (Eds.), *Stem Cell Biology and Tissue Engineering in Dental Sciences* (42, 553–565), Elsevier Inc. https://doi.org/https://doi.org/10.1016/B978-0-12-397157-9.00076-X

Denchai, A., Tartarini, D., & Mele, E. (2018). Cellular Response to Surface Morphology: Electrospinning and Computational Modeling. *Front. Bioeng. Biotechnol.*, ***6***(October), 1–11. https://doi.org/10.3389/fbioe.2018.00155

Goulet, F., Auger, F. A., Cloutier, R., Lamontagne, J., Simon, F., Chabaud, S., Germain, L., Hart, D. A. (2014). Tendons and Ligament Tissue Engineering. In R. Lanza, R. Langer, & J. Vacanti (Eds.), *Principles of Tissue Engineering* (59, 1275–1287). Elsevier Inc. https://doi.org/10.1016/B978-0-12-398358-9.00059-8

Hampson, K., Forsyth, N. R., El Haj, A., & Maffulli, N. (2008). Tendon Tissue Engineering. In N. Ashammakhi, R. Reis, & F. Chiellini (Eds.), *Topics in Tissue Engineering* (3, 1–21). https://www.oulu.fi/spareparts/ebook_topics_in_t_e_vol4/abstracts/hampson.pdf

Kannus, P. (2000). Structure of the tendon connective tissue. *Scand. J. Med. Sci. Sport.*, ***10***(6), 312–320. https://doi.org/10.1034/j.1600-0838.2000.010006312.x

Kastelic, J., Galeski, A., & Baer, E. (1978). The Multicomposite Structure of Tendon. *Connect. Tissue Res.*, ***6***(1), 11–23. https://doi.org/10.3109/03008207809152283

Kuo, C. K., Marturano, J. E., & Tuan, R. S. (2010). Novel strategies in tendon and ligament tissue engineering : Advanced biomaterials and regeneration motifs. *Sport. Med. Arthrosc. Rehabil. Ther. Technol.*, ***2***(20), 1–14.

Leferink, A. M., Van Blitterswijk, C. A., & Moroni, L. (2016). Methods of Monitoring Cell Fate and Tissue Growth in Three-Dimensional Scaffold-Based Strategies for In Vitro Tissue Engineering. *Tissue Eng. Part B Rev.*, ***22***(4), 1–19. https://doi.org/10.1089/ten.teb.2015.0340

Liu, Z. (1991). Scale space approach to directional analysis of images. *Appl. Opt.*, ***30***(11), 1369–1373. https://doi.org/https://doi.org/10.1364/AO.30.001369

Murphy, W., Black, J., & Hastings, G. (2016). *Handbook of Biomaterial Properties*. (W. Murphy, J. Black, & G. Hastings, Eds.) (Second). Springer. https://doi.org/10.1007/978-1-4939-3305-1

Schindelin, J., Arganda-Carreras, I., Frise, E., Kaynig, V., Longair, M., Pietzsch, T., …

519 Cardona, A. (2012). Fiji: an open-source platform for biological-image analysis.
520 *Nat. Methods*, ***9***(7), 676–682. https://doi.org/10.1038/nmeth.2019
521 Schneider, C. A., Rasband, W. S., & Eliceiri, K. W. (2012). NIH Image to ImageJ: 25
522 years of image analysis. *Nat. Methods*, ***9***(7), 671–675.
523 https://doi.org/10.1038/nmeth.2089
524 Sensini, A., Cristofolini, L., Focarete, M. L., Belcari, J., Zucchelli, A., Kao, A., &
525 Tozzi, G. (2018). High-resolution x-ray tomographic morphological
526 characterisation of electrospun nanofibrous bundles for tendon and ligament
527 regeneration and replacement. *J. Microsc.*, ***272***(3), 196–206.
528 https://doi.org/10.1111/jmi.12720
529 Sensini, A., & Cristofolini, L. (2018). Biofabrication of Electrospun Scaffolds for the
530 Regeneration of Tendons and Ligaments. *Materials (Basel).*, ***11***(10), 1963.
531 https://doi.org/10.3390/ma11101963
532 Sensini, A., Cristofolini, L., Gualandi, C., Focarete, M. L., Belcari, J., & Zucchelli, A.
533 (2018). *WO 2018/229615 A1*.
534 Sensini, A., Gotti, C., Belcari, J., Zucchelli, A., Focarete, M. L., Gualandi, C., Todaro,
535 I., Kao, A. P., Tozzi, G., Cristofolini, L. (2019). Morphologically bioinspired
536 hierarchical Nylon 6.6 electrospun assembly recreating the structure and
537 performance of tendons and ligaments. *Med. Eng. Phys.*
538 Sensini, A., Gualandi, C., Cristofolini, L., Tozzi, G., Dicarlo, M., Teti, G., Mattioli-
539 Belmonte, M., Focarete, M. L. (2017). Biofabrication of bundles of poly(lactic
540 acid)-collagen blends mimicking the fascicles of the human Achille tendon.
541 *Biofabrication*, ***9***(1). https://doi.org/10.1088/1758-5090/aa6204
542 Sensini, A., Gualandi, C., Focarete, M. L., Belcari, J., Zucchelli, A., Boyle, L., Reilly,
543 G. C., Kao, A. P., Tozzi, G., Cristofolini, L. (2019). Multiscale hierarchical
544 bioresorbable scaffolds for the regeneration of tendons and ligaments.
545 *Biofabrication*, ***11***(3), 35026. https://doi.org/10.1088/1758-5090/ab20ad
546 Sensini, A., Gualandi, C., Zucchelli, A., Boyle, L., Kao, A. P., Reilly, G. C., Tozzi, G.,
547 Cristofolini, L., Focarete, M. L. (2018). Tendon Fascicle-Inspired Nanofibrous
548 Scaffold of Polylactic acid/Collagen with Enhanced 3D-Structure and
549 Biomechanical Properties. *Sci. Rep.*, ***8***(1), 1–15.
550 https://doi.org/https://doi.org/10.1038/s41598-018-35536-8
551 Tseng, L. F., Mather, P. T., & Henderson, J. H. (2013). Shape-memory-actuated
552 change in scaffold fiber alignment directs stem cell morphology. *Acta Biomater.*,
553 ***9***(11), 8790–8801. https://doi.org/10.1016/j.actbio.2013.06.043
554 Wu, S., Wang, Y., Streubel, P. N., & Duan, B. (2017). Living nanofiber yarn-based
555 woven biotextiles for tendon tissue engineering using cell tri-culture and
556 mechanical stimulation. *Acta Biomater.*, ***62***, 102–115.
557 https://doi.org/10.1016/j.actbio.2017.08.043
558 Xu, Y., Dong, S., Zhou, Q., Mo, X., Song, L., Hou, T., Wu J., Li, S., Li, Y., Li, P.,
559 Gan, Y., Xu, J. (2014). The effect of mechanical stimulation on the maturation of
560 TDSCs-poly(L-lactide-co-e-caprolactone)/collagen scaffold constructs for tendon
561 tissue engineering. *Biomaterials*, ***35***(9), 2760–2772.
562 https://doi.org/10.1016/j.biomaterials.2013.12.042
563 Youngstrom, D. W., & Barrett, J. G. (2016). Engineering tendon: Scaffolds,
564 bioreactors, and models of regeneration. *Stem Cells Int.*, ***2016***, 1–12.
565 https://doi.org/10.1155/2016/3919030
566 Zidek, J., Vojtova, L., Abdel-Mohsen, A. M., Chmelik, J., Zikmund, T., Brtnikova, J.,
567 Jakubicek, R., Zubal, L., Jan, J., Kaiser, J. (2016). Accurate micro-computed
568 tomography imaging of pore spaces in collagen-based scaffold. *J. Mater. Sci.*

569 *Mater. Med.*, ***27***(6), 1–18. https://doi.org/10.1007/s10856-016-5717-2
570
571

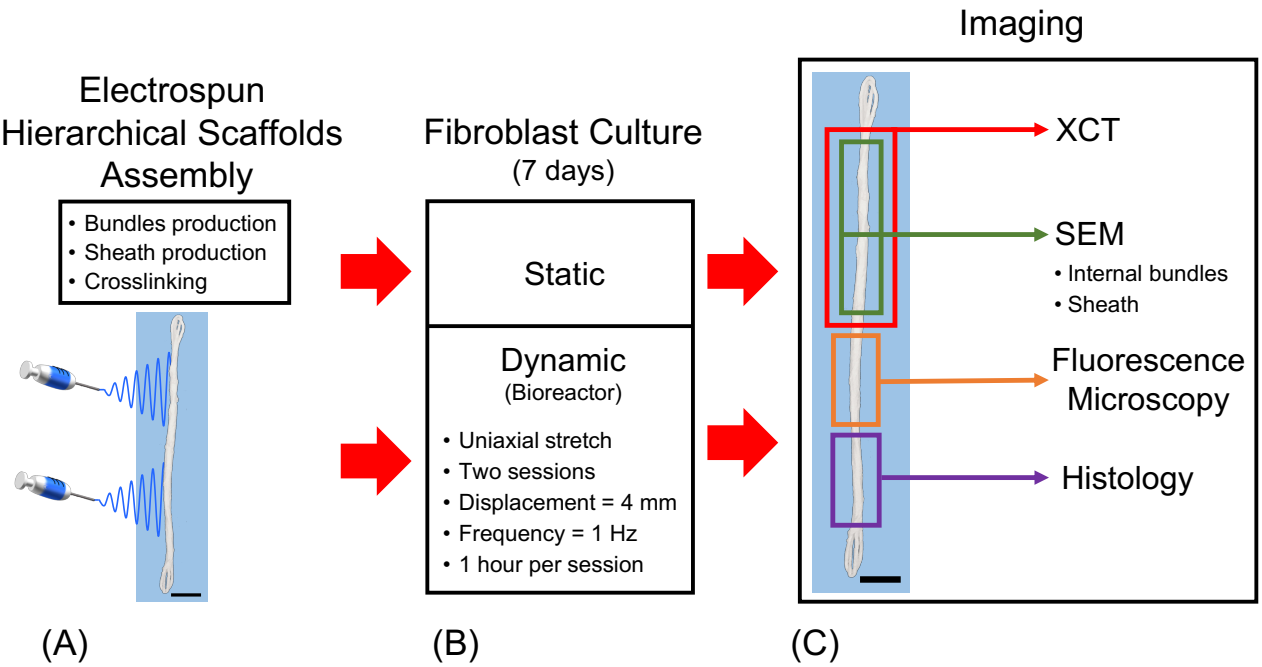

Fig. 1. Workflow of the experiment. (A) Electrospun hierarchical scaffolds assembly (scale bar = 1 mm). (B) Fibroblasts culture: two scaffolds were cultured in static conditions, while other two with uniaxial sessions of stretching in a bioreactor. (C) Scaffolds preparation for the different imaging investigations (scale bar = 1 mm).

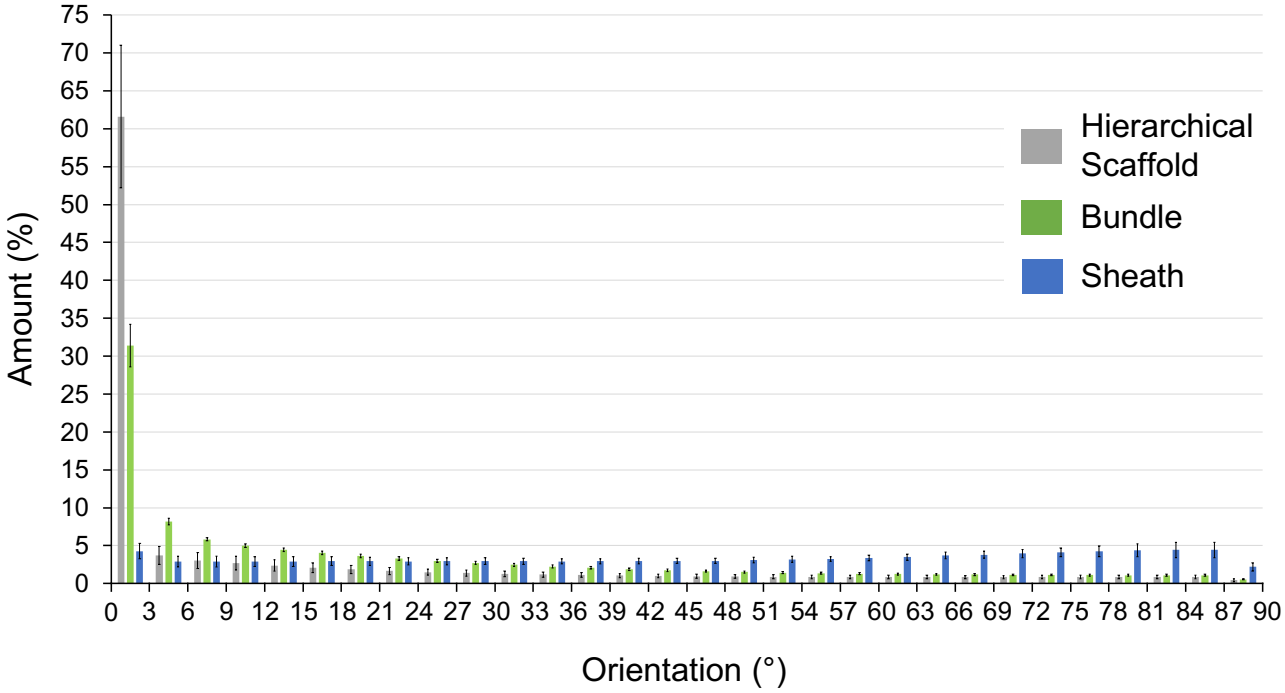

Fig. 2. Directionality analysis at different levels of the hierarchical scaffolds. The directionality histograms show the comparison between: the alignment of the bundles inside the hierarchical scaffold (gray bars), the distribution of nanofibers in the different directions for the bundle (green bars) and on the electrospun sheath (blue bars). An angle of 0° means that the nanofibers were aligned with the longitudinal axis of the hierarchical scaffold, an angle of 90° means that the nanofibers were perpendicular to it. Mean and standard deviation between images of the same specimen are plotted.

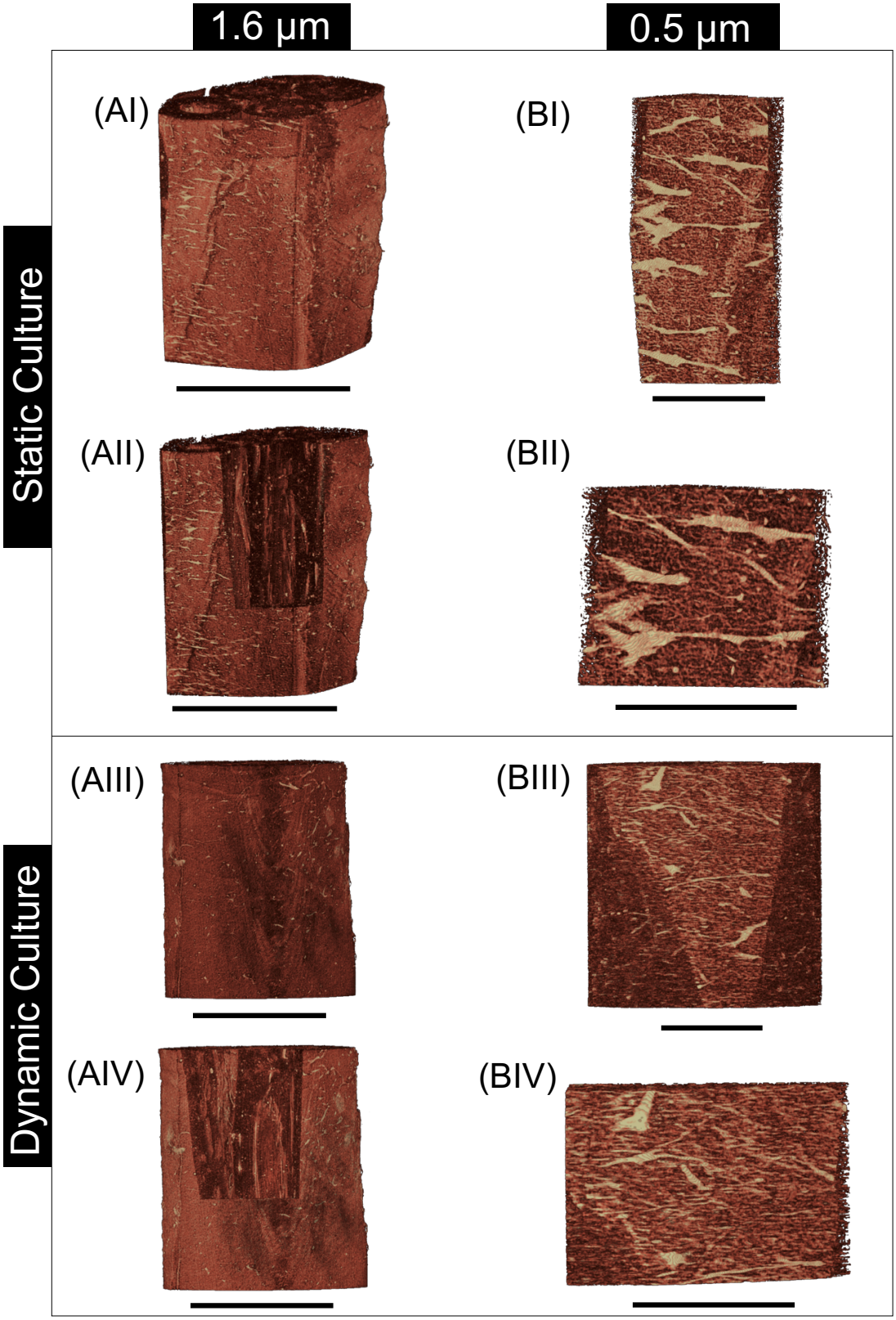

Fig. 3. XCT images of fibroblasts cultured onto the hierarchical scaffolds in static (I, II) and dynamic (III, IV) conditions. (AI, III) Overview of the scaffolds; (AII, IV) superficial crop showing the internal bundles (voxel size = 1.6 micrometers; scale bar =1 mm). (BI, III) Overview of fibroblasts on the external sheath; (AII, IV) zoom on the fibroblasts (voxel size = 0.5 micrometers; scale bar = 200 micrometers).

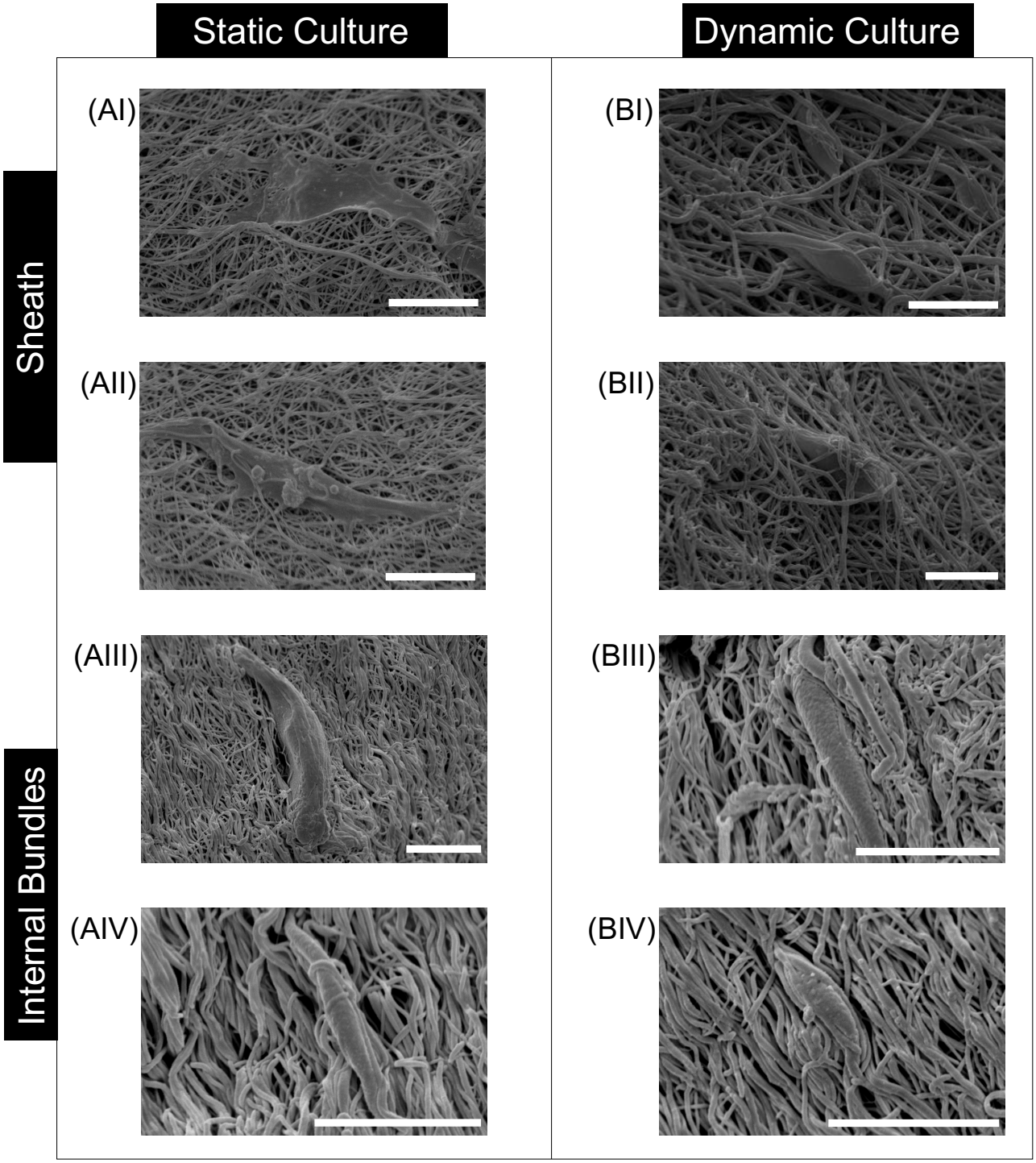

592
593 **Fig. 4.** SEM images of fibroblasts cultured onto the hierarchical scaffolds in static (A)
594 and dynamic (B) conditions (scale bar = 10 micrometers). (I-II) SEM images of the
595 fibroblasts on the electrospun sheath; (III-IV) SEM fibroblasts on the internal bundles.

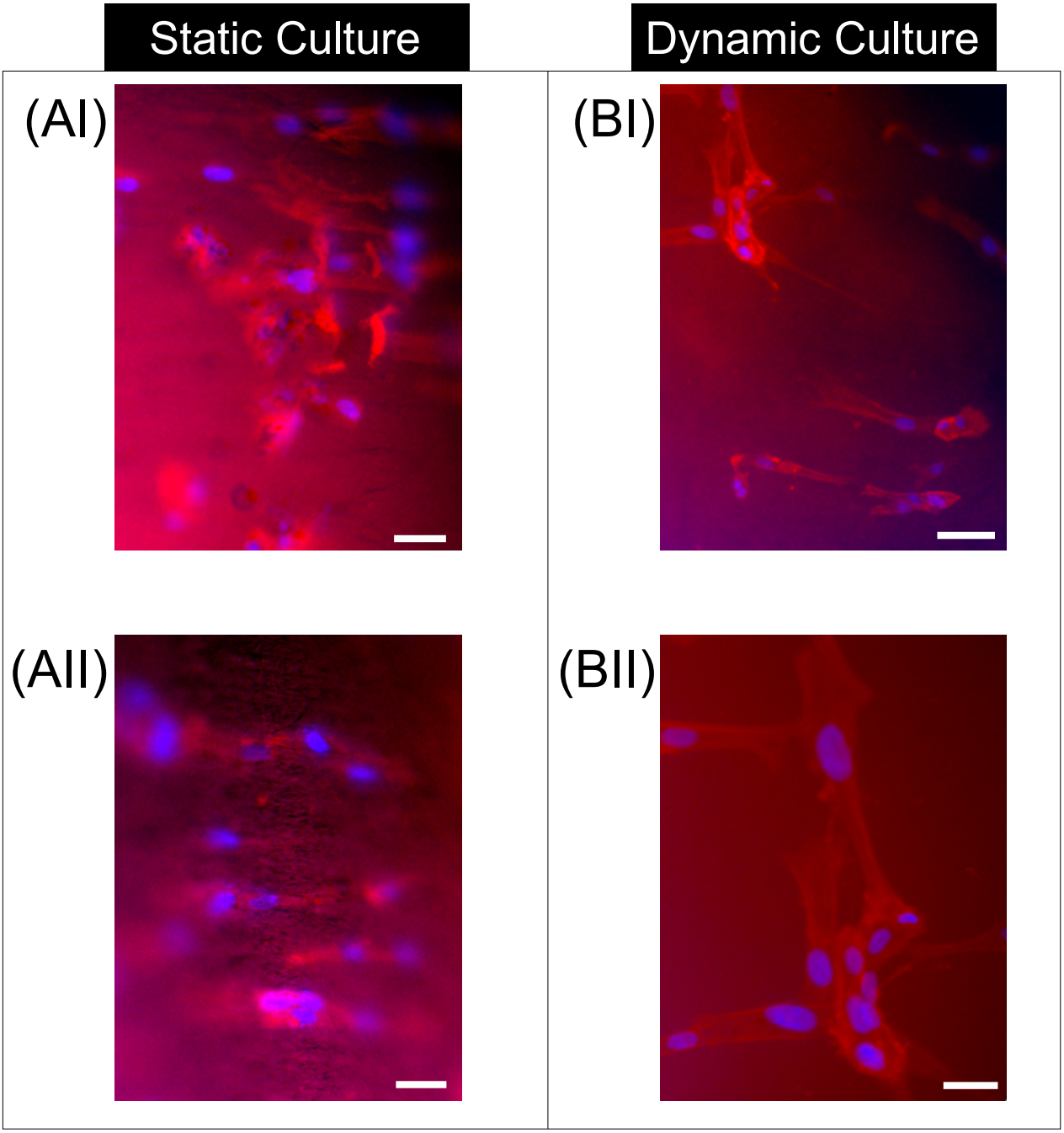

Fig. 5. Fluorescence images of fibroblasts onto the hierarchical scaffolds sheath in static (A) and dynamic (B) conditions (scale bar = 30 micrometers).

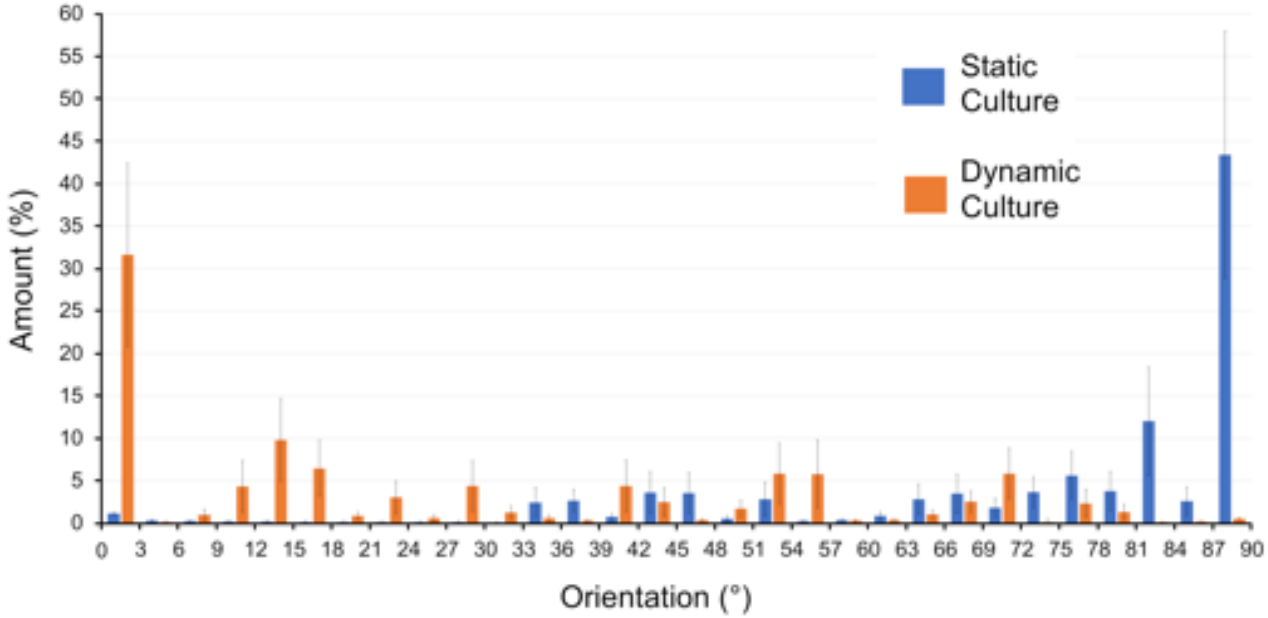

Fig. 6. Directionality analysis of cells grown on the electrospun sheaths (based on the orientation of the cells nuclei) in static and dynamic conditions of culture. An angle of 0° means that the cells were aligned with the longitudinal axis of the hierarchical scaffold, an angle of 90° means that the cells were perpendicular to it. Mean and standard deviation between images of the static and dynamic specimens are plotted.

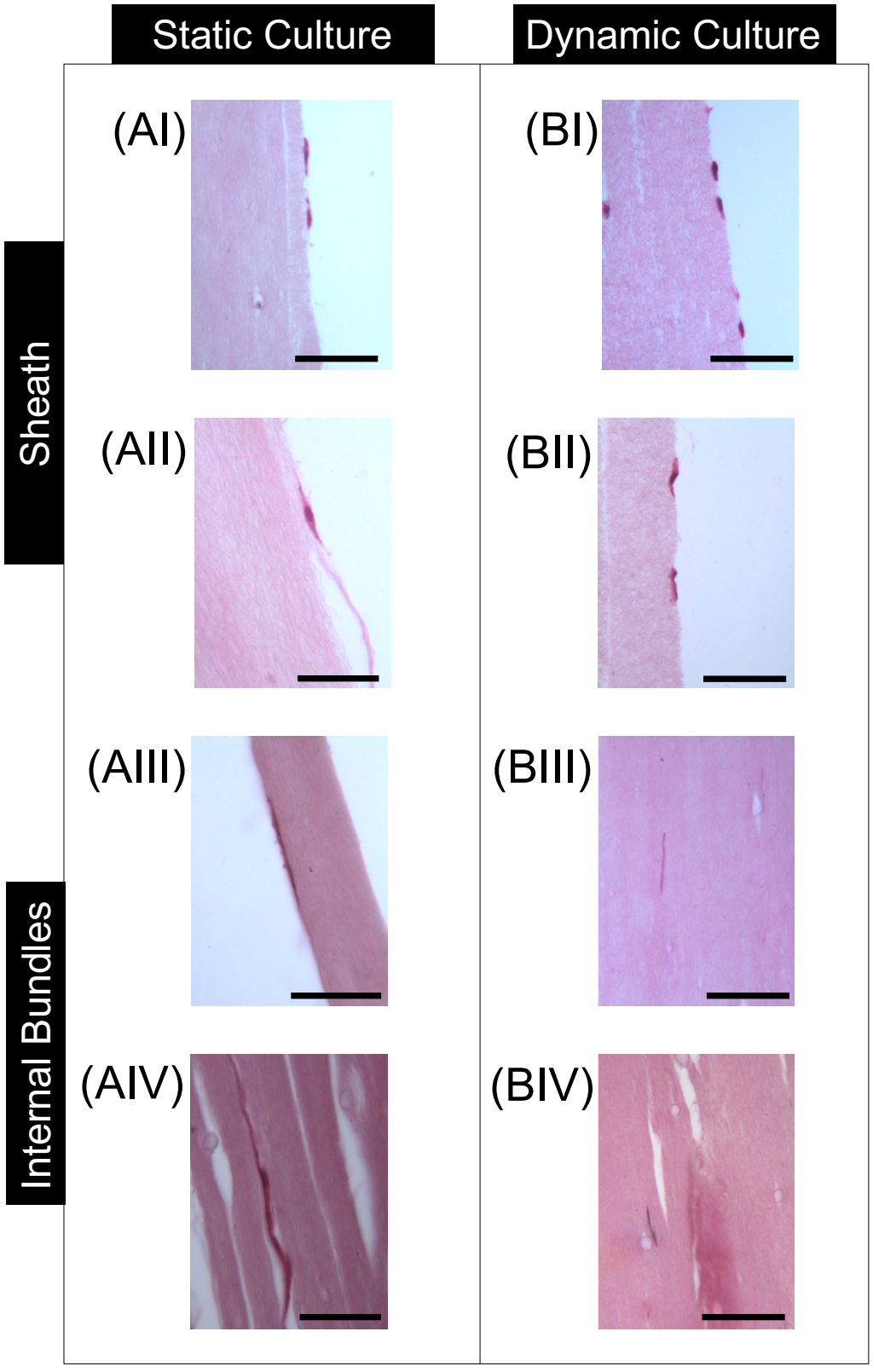

606

607 **Fig. 7.** Histological investigation on the hierarchical scaffolds cultured in static (A) and
608 dynamic (B) conditions (scale bar = 50 micrometers). (I-II) Zoom-in on the fibroblasts
609 on the electrospun sheath; (III-IV) images of the elongated fibroblasts on the aligned
610 nanofibers of the internal bundles.
611